Supporting information

Synthesis, Characterization and Bio-conjugation of Fluorescent Gold Nanoclusters towards Biological Labeling Applications

Cheng-An J. Lin[1,5], Ting-Ya Yang[1,5], Chih-Hsien Lee[1,5], Sherry H. Huang[1,5], Ralph A. Sperling[2], Marco Zanella[2], Jimmy K. Li[1,5#], Ji-Lin Shen[3], Hsueh-Hsiao Wang[3], Hung-I Yeh[3], Wolfgang J. Parak[2], Walter H. Chang[1,5]**

[1] Department of Biomedical Engineering, Chung Yuan Christian University, Chung-Li 32023, Taiwan (R.O.C.)
[2] Fachbereich Physik, Philipps Universität Marburg, Renthof 7, 35037 Marburg (Germany)
[3] Department of Physics, Chung Yuan Christian University, Chung-Li 32023, Taiwan (R.O.C.)
[4] Cardiac Medicine, Mackay Memorial Hospital, Taipei, Taiwan (R.O.C.)
[5] R&D Center for Membrane Technology, Center for Nano Bioengineering, Chung Yuan Christian University, Chung-Li 32023, Taiwan (R.O.C.)
[#] Present address: Harvard–MIT Health Sciences and Technology, Brigham and Women's Hospital, Harvard Medical School, Cambridge, MA, 02139

*Corresponding author:
Prof. Walter H. Chang, email: whchang@cycu.edu.tw;
Prof. Dr. Wolfgang Parak, email: Wolfgang.Parak@physik.uni-marburg.de

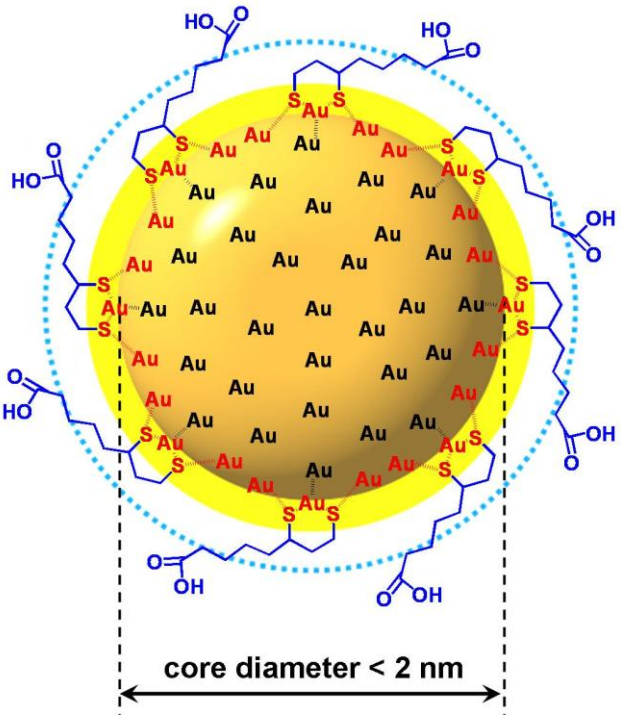

~Table of Contents~

Supporting Methods:

Supporting Figures:

Supporting Methods:

SI.1: Synthesis of fluorescent Au nanoclusters (AuNC@DHLA)

SI.1-1 General description

We introduce a general approach to make small gold nanoparticles or nanoclusters (NCs) in organic phase. For this purpose gold nanoparticles prepared from a one-phase reaction either with or without purification by methanol precipitation are etched into small NCs by the gold precursor solution. The etched gold NCs lose their surface plasmon properties and lead to a yellowish or even colorless transparent solution, whereas the original larger gold nanoparticles possess strong surface plasmon absorption around 520~530 nm. The addition of freshly reduced lipoic acid can replace the surfactants on the etched gold NCs via the formation of strong dithiol-Au bonds, whereby the acid headgroup points towards the solution. Upon such ligand exchange with lipoic acid the gold NCs become red-emitting fluorophores. By deprotonization under basic buffer, the etched gold NCs become water-soluble and form a mono-dispersion stabilized by electrostatic repulsion.

SI.1-2 Chemicals

Didodecyldimethylammonium bromide (DDAB, >98% purity; Fluka), decanoic acid (>98% purity, Aldrich), tetrabutylammonium borohydride (TBAB, >97% purity, Fluka), gold (III) chloride (AuCl3, 99% purity, Strem Chemicals), gold (III) chloride trihydrate ($HAuCl_4.3H_2O$), (±)-α-lipoic acid (≥99% purity, Sigma), toluene (Sigma).

SI.1-3 Etched gold nanoclusters (NCs) derived from gold nanoparticles (NPs)

The synthesis of 6 nm gold nanoparticles was adopted from Peng's protocol for a single-phase reaction[1]. The small gold nanoclusters were then derived by etching the initial gold nanoparticles by the Au precursor solution. In brief, appropriate amounts of DDAB or decanoic acid were dissolved in toluene as stock solution of 100 mM concentration. Gold precursor solution (25 mM) was then prepared by dissolving an appropriate amount of gold(III) chloride ($AuCl_3$ or $HAuCl_4$) in the DDAB solution. In a typical synthesis, 1 ml of fresh-prepared TBAB solution (100 mM in 1DDAB stock solution,) was firstly mixed with 0.625 ml decanoic acid stock solution under vigorous stirring. Then 0.8 ml gold precursor solution was injected under vigorous stirring leading instantaneously to a dark-red solution of Au nanoparticles. After two hours reaction, the gold nanoparticles were collected by methanol-induced agglomeration, i.e. by adding excess methanol until obtaining a blue-purple cloudy solution. Free surfactants, reduction agents and smaller nanoparticles were removed by discarding

the supernatants of this solution by centrifugation (2500 rpm, 30 min). The wet precipitate of Au nanoparticles was then re-dissolved in 2.5 ml DDAB stock solution, yielding a dark blood-red color (AuNP@DDAB). Upon addition of several drops of gold precursor solution under vigorous stirring, the solution color turned from dark-red color to a yellowish transparent solution. This change in color was quantified with UV/vis absorption spectroscopy (**Figure S1**). The data indicate vanishing of surface plasmon absorption around 520~530 nm, what we attribute to the etching or fragmenting of Au nanoparticles to smaller Au nanoclusters (AuNC@DDAB).

The etching or fragmenting process induced by gold precursors has been verified to be similar for different gold precursors, such as $AuCl_3$, $HAuCl_4$, $AuBr_3$, and $HAuBr_4$. The addition of only a little amount of gold precursor solution is enough to lead to vanishing of the surface plasmon absorption. Etching (observed by vanishing of the surface plasmon absorption) could be also observed in the case when the particles were not precipitated and purified with methanol before adding the gold precursor solution. However, in this case the plasmon absorption increased in the beginning upon precursor addition, likely due to the residue of active reducing agents still in solution (i.e. TBAB), which resulted in growing of the nanoparticles. Upon exhaustion of the reducing agents (which reduce gold precursors to Au nanoparticles), the plasmon peak started to decrease upon further addition of new Au precursor solution and eventually vanished (**Figure S2**). Therefore, when the gold particles were not purified prior the addition of Au precursor, the more gold precursor needed to be added for the etching of the nanoparticles until a final transparent solution was obtained.

SI.1-4 Fluorescent gold nanoclusters obtained by ligand-exchange

The as-prepared gold nanoclusters (AuNC@DDAB) are not fluorescent, except the case when $AuCl_3$ was used as gold precursor for the etching process. Au nanoclusters etched with $AuCl_3$ exhibited weak blue emission upon UV excitation in case the excess precursors were not removed. In this way the initial weak blue fluorescence can be attributed to impurities and does not originate form the Au. All gold nanoclusters (either etched with $HAuCl_4$ or $AuCl_3$ precursor solution) became red fluorescent upon ligand exchange by dithiol. By using polar dithiols the gold nanoclusters were rendered water-soluble upon ligand exchange. First, 0.0322 g of TBAB powder and 2.5 ml of DDAB solution in toluene were mixed into a 8 ml vial until no solid powders remained. The mixture was then transferred into another vial containing 0.052 g of lipoic acid (LA) powder and stirred until no more bubbles were generated. In this step lipoic acid is reduced into dihydrogenlipoic acid (DHLA). Residual active TBAB can also cause the growing of nanoclusters even upon ligand exchange, giving again non-fluorescent nanoclusters. To eliminate residual activity of the TBAB reducing agent, another 0.052g

of lipoic acid powder were again added in excess[i] into the reduced lipoic acid mixture and stirred until no more bubbles were generated before running the ligand exchange. In this way the final molar ratio of LA/TBAB was 4/1.

Freshly-reduced lipoic acid (DHLA) contains two free thiol groups per molecule which are reactive towards the surfaces of the gold nanoclusters, whereas the oxidized forms of lipoic acids did not show to react when added into solutions of etched gold nanocluster. 2.5 ml of etched gold nanoclusters were quickly loaded into the equal amount of DHLA solution in toluene under vigorous stirring. The solution turned cloudy immediately and formed a yellow-brown agglomeration due to ligand exchange. After 10 min of stirring the cloudy solution was then placed onto an UV-exposure box (UVP, U.K.) and exposed to UV-light (365 nm) for 20 - 30 min. The nanoclusters agglomerates gradually became red-fluorescent upon UV exposure, which could be observed by naked eye (**Figure S3**). UV exposure also stimulated the formation of more compact agglomerates. After removing the supernatant (which includes free surfactants) the brown precipitate of DHLA-capped Au nanoclusters (AuNC@DDAB) was washed two times by toluene and finally re-dissolved in methanol. All solvents were then evaporated under reduced pressure by a rotavapor system (Laborota 4000, Heidolph). Then 2 ml of chloroform were carefully added to the nanoclusters to remove remaining free surfactant molecules, the supernatant was discarded[ii] and the particle precipitate was dried again under reduced pressure. Addition of 5 ml of 0.1 M NaOH caused deprotonation of the COOH groups of the dried AuNC@DHLA and thus rendered the nanoclusters soluble in the water phase[iii]. Several purification steps followed. Filtration through a syringe membrane filter (Roth # P818.1, 0.22 μm pore size) helped to remove any remaining particle aggregates from solution. The gold nanoclusters were also purified by passing through the membrane of a 100 kDa MWCO centrifuge filter (Millipore) and the particles were concentrated and finally collected by a 30 kDa MWCO centrifuge filter. The buffer could be changed via several runs of dilution and concentration cycles by the centrifuge filter if necessary. Alternatively, the larger aggregates in the nanocluster solutions could be removed by precipitation with centrifugation (usually 10,000 r.p.m. for 30 mins) and all the fluorescent gold nanoclusters were then precipitated (two times) with centrifugation at higher speed (usually 110,000 r.p.m. for 4 hours), which allowed for removing possible residues of free surfactant by discarding the supernatant.

SI.2: Size characterization of fluorescent Au nanoclusters:

The size distribution of the fluorescent Au nanoclusters was characterized by several techniques: transmission electron microscopy (TEM), size exclusion chromatography (SEC), atomic force microscopy (AFM) and gel electrophoresis[2].

TEM was used for visualizing the shape as well as measuring the diameter of the inorganic Au particles. TEM images were with a JEOL electron microscope operated at an accelerating voltage of 200 kV. The as-prepared gold nanoparticles (AuNP@DDAB) as well as the precursor-etched Au nanoclusters (AuNC@DDAB) were directed dried on carbon supported copper grids (#01822-F ultra-thin carbon type–A from Ted Pella Inc.). In case of DHLA-capped Au nanoclusters (AuNC@DHLA) the particles were first dissolved in methanol prior to depositing them on the TEM grids. The average size distribution of particles was determined from the TEM images by using the image analysis software "ImageJ" which is available at the NIH website http://rsb.info.nih.gov/ij/. 100 particles per image were selected for statistic analysis. The results from the TEM analysis are shown in **Figure S4**. The as-prepared Au nanoparticles (AuNP@DDAB) had a core diameter of 5.55±0.68 nm. The sequential addition of Au precursors into the Au nanoparticles resulted in disappearance of the plasmon absorption (see. SI.1-3), which is due to the etching of the particles. TEM images recorded on the resulting Au nanoclusters (AuNC@DDAB) indicate a diameter of 3.17±0.35 nm. Performing ligand exchange using DHLA on the Au nanoclusters further reduced the nanoclusters size to 1.56±0.3 nm (AuNC@DHLA). The Au nanoclusters were also found to be crystalline.

The hydrodynamic diameter of the Au nanoclusters (AuNC@DHLA) was determined with size exclusion chromatography using a Sephacryl S-200 column. Methoxy-polyethylene glycol (mPEG, Rapp Polymere) of different molecular weight was used as standards[3] to correlate the elution time with the hydrodynamic diameter[iv]. The hydrodynamic diameter includes the size of the inorganic core[v] plus two times the thickness of the organic shell around it. The data are presented in **Figure S5**. The Au nanoclusters elute at the same time like PEG molecules of 1 - 3 kDa molecular weights, with the peak coinciding with the 3 kDa PEG. This corresponds to hydrodynamic diameters ranging from 1.28 nm - 3.36 nm.

Gel electrophoresis was used as additional method to investigate the hydrodynamic diameter. The lager the nanoparticles are, the slower their mobility is[vi]. Two types of hydrophobic nanoparticles were then transferred into aqueous phase by capping them with reduced lipoic acid (DHLA)[vii]: the original Au nanoparticles before etching (AuNP@DHLA) and the Au nanoclusters after etching[viii] (AuNC@DHLA). As reference 10-nm and 5-nm colloidal gold nanoparticles (BBInternational) coated with bis(p-sulfonatophenyl)phenylphosphine (Strem) were run simultaneously on the same

gel. Gel electrophoresis was performed with 2% agarose gels for 20 mins (7.5 V/cm, Sub-Cell GT electrophoresis cells, Bio-Rad). Gel images were taken with a Pentax Optio mx4 camera, whereby the fluorescence images were recorded with UV excitation (365 nm) and the UV background was later removed using the software Photoimpact-v.12. The results are shown in **Figure S6**. The small fluorescent Au nanoclusters (AuNC@DHLA) were running faster than the larger Au nanoparticles also capped with DHLA. While the Au nanoclusters were emitting red fluorescence, there was no detectable fluorescence found in the case of the larger gold nanoparticles, even when they were capped with the same molecule (i.e. DHLA).

SI.3: Optical properties of fluorescent Au nanoclusters:

SI.3-1 UV/vis Absorption Spectra

Reduction of surface plasmon absorption upon addition of Au precursors was recorded by UV/vis spectroscopy (Varian Cary 50)[ix]. Addition of Au precursors (i.e. $AuCl_3$ or $HAuCl_4$ in DDAB solution) etched 6-nm gold nanoparticles (AuNP@DDAB) into small nanoclusters[x] (AuNC@DDAB). UV/vis absorption spectra demonstrate the vanishing of plasmon absorption of the Au nanoparticle at 520~530 nm upon the etching process (**Figure S7**). The hydrophobic Au nanoparticles and the Au nanoclusters which are stabilized with DDAB surfactants were then dispersed into aqueous solution via ligand exchange with DHLA. The DHLA-capped Au nanoparticles (AuNP@DHLA) showed a blue-shifted plasmon peak, indicating reduced sizes compared to the original DDAB-stabilized Au nanoparticles[xi]. Interestingly, the DHLA-capped Au nanoclusters (AuNC@DHLA) showed an elevated absorption in the UV/vis range compared to the DDAB-stabilized Au nanoclusters.

SI.3-2 Photoluminescence (PL) and Photoluminescence Excitation (PLE)

No detectable photoluminescence was found for gold nanoparticles and nanoclusters in organic as well as in aqueous phase except for the case of DHLA-capped nanoclusters [xii]. DHLA-capped nanoclusters exhibited red photoluminescence. Dependence of the fluorescence on the ligand indicates that the surface plays a role in the fluorescence properties. In case of DHLA capped nanoclusters thiol-gold bonds (R-S-Au··Au-S-R) are present on the particle surface. Also size plays a crucial role, as fluorescence was found for small DHLA-capped Au nanoclusters, but not for the bigger DHLA-capped Au nanoparticles. This suggest that for being fluorescent Au particles need to be capped with DHLA and they also need to be small enough (less than 2 nm in this work). PL & PLE spectra of fluorescent Au nanoclusters dispersed in aqueous phase were first measured by fluorescence spectrometer (FP-6200, JASCO) as shown in **Figure S8a**. The fluorescent AuNC@DHLA emitted a similar emission profile regardless the excitation wavelength (350, 400, 450, and 490 nm). The PLE of diluted solutions of fluorescent AuNC@DHLA was recorded at fixed wavelength of emission (630 nm) and spectra were normalized with the related excitation intensity. Data indicate that fluorescent AuNC@DHLA possess a broad excitation range from the UV to the green. Due to the poor sensitivity as well as the limited detection range of the JASCO spectrometer in the near infrared, an additional fluorescence spectrometer with better sensitivity (Fluorolog-3, Jobin Yvon) was applied for comparing the emission profile of the same samples (**Figure S8b**).

Also solid-state PL & PLE fluorescence spectra were recorded (**Figure S9**). For this

purpose fluorescent Au NCs dispersed in methanol were dried on a coverslip to form a thick particle layer. PL, which is a nondestructive optical technique, is a convenient method to analyze the optical properties of nano-materials. PL can be used to characterize a variety of material parameters, and provides information on the impurity levels and the quality of surfaces and interfaces. Another useful technique to investigate the physical nature of luminescence signal is PLE, which measures the excited levels or bands of the system by detecting the photon energy at emission band. In the PLE mechanism, the luminescence intensity is proportional to the number of photogenerated carriers, which is in turn proportional to the absorption. The PL spectra were measured using a GaN diode laser (396 nm) with a pulse duration 50 ps as the excitation source. PLE measurements were carried out with broad band light from a Xe lamp passing a grating monochromator. The collected luminescence was dispersed by a grating spectrometer and detected with a cooled GaAs photomultiplier tube.

SI.3-3 Quantum Yield

Fluorescence quantum yield is defined as the numbers of emitted photons per number of absorbed photons. Quantum yields are typically measured by a relative comparison method[4]:

$$\frac{Q_t}{Q_s} = \frac{I_t A_s \eta_t^2}{I_s A_t \eta_S^2} = \frac{\left(\frac{I_t}{A_t}\right)\eta_t^2}{\left(\frac{I_s}{A_s}\right)\eta_S^2}$$

Q=Quantum Yield; t= Test Sample; S= Standard Sample; η= Refractive index of solvent; A= Absorption at the selected excitation wavelength

To calculate the quantum yield absorption and fluorescence spectra of concentration series of the test sample and a reference sample (with known quantum yield) were measured. In order to avoid artifacts solutions should have optical densities between 0.1 and 0.01. Here, Rhodamine 6G dissolved in ethanol (Q=0.95) was used as standard. Fluorescent gold nanoclusters (AuNC@DHLA) dispersed in methanol as well as in alkaline aqueous solution (0.1 N NaOH) were used. For each sample and concentration the absorption (optical density) at 480 nm (Varian Cary 50) and the corresponding photoluminescence spectra (Fluorolog-3, Jobin Yvon) were recorded. The intensity versus absorption gradients of each sample was linearly fitted. After correction with the refractive index of each solvent the quantum yield of the test sample could be determined by using the formula above. The quantum yield of fluorescent gold

nanoclusters was determined as 3.45±0.41% in methanol and as 1.83±0.32% in aqueous phase. (**Figure S10**)

SI.3-4 Photostability

Photostability was probed by recording the intensity change emitted fluorescent upon continuous photoexcitation. Traditional organic fluorophores such as fluorescein suffer from fast photobleaching upon optical excitation. Core/shell quantum dots (e.g. CdSe/ZnS) have been demonstrated to possess high photostability (i.e. low photobleaching). Here we compare the photostability of fluorescent Au NCs with two organic fluorophores (Rhodamine 6G, fluorescein) as well as with one quantum dot sample. Rhodamine 6G and fluorescein (Sigma) were dissolved in sodium borate buffer (SBB, pH 9). Hydrophobic quantum dots (QD520, Evident Technology) were coated with an amphiphilic polymer (75% dodecylamine-modified poly(isobutyl-maleic anhydride)) and dissolved in SBB solution[5]. Fluorescent gold nanoclusters (AuNC@DHLA) were also prepared in SBB solution as shown in SI.1-4. All samples were first adjusted to equal optical density (0.08) at 480 nm before recording their photostability. Fluorescence spectra were recorded every second by a fluorescence spectrometer (Fluorolog-3, Jobin Yvon) equipped high-power Xenon lamp and the intensities were plotted versus time. The excitation bandwidth was set to 20 nm and samples were loaded loaded into small cuvettes (20 μl capacity). As shown in **Figure S11**, semiconductor quantum dots (CdSe/ZnS) showed an excellent photostability and did not photobleach within the observation time. Fluorescent AuNC@DHLA photobleached faster than quantum dots but still much slower than traditional organic fluorophores.

SI.4: Bioconjugation of fluorescent Au nanoclusters

To prove the bioconjugate capability of the fluorescent AuNC@DHLA as synthesized in this work, polyethylene glycol (PEG), biotin and avidin were selected as examples for bioconjugation. As shown in **Figure S12a**, water-soluble fluorescent AuNC@DHLA are covalently capped by dihydrolipoic acid (DHLA) via thiol-Au bonds. The carboxylic acids on the end of DHLA pointing towards solution are the origin of the negative surface charges of the particles. They also can be used for conjugation with functional moieties. PEG molecules have been widely used in biomedicine due to their excellent biocompatibility as well as their versatile terminals. X-PEG-amines (X-PEG-NH2, X= methoxy, biotin, etc.), for example, are ready to couple with the carboxylic groups present on the surface of water-soluble fluorescent Au nanoclusters as shown in **Figure S12b** and **Figure S12c**. 1-Ethyl-3-[3-dimethylaminopropyl] carbodiimide (EDC) was used as crosslinking agent between carboxyl groups and primary amines. EDC forms an amine-reactive *O*-acylisourea intermediate with carboxyl groups and mediates amide bond formation upon encountering primary amines.

For linkage with PEG, purified fluorescent AuNC@DHLA were concentrated to 15 μM in SBB (pH 9) solution[xiii]. 3 mM of X-PEG-amine (methoxy-PEG5k-NH_2 or biotin-PEG5k-NH_2 from Rapp Polymer, Germany) was prepared in double distilled water. 8 mM EDC (Sigma) was prepared in double distilled water and aliquoted in seven fractions out of which each one had half of the EDC concentration as the previous one. Dissolved EDC (10 μl) was added to a mixture containing fluorescent AuNC@DHLA (10 μl) and X-PEG-amine (10 μl). After two hours of reaction, the fluorescent Au nanoclusters were run through gel electrophoresis with a 2% agarose gel (20 min, 7.5V/cm, Sub-Cell GT electrophoresis cells, Bio-Rad). Images of the gels were taken with a Pentax Optio mx4 camera. Fluorescence images were collected under 365 excitation and UV background removal using Photoimpact-v.12 software. As shown in **Figure S13a**, EDC at higher concentration (i.e. 16 mM) caused a slight retardation of the fluorescent AuNC@DHLA event without the presence of PEG-amine. This could be due to that EDC forms some semi-stable *O*-acylisourea intermediate on the surface of fluorescent AuNC@DHLA. However, discrete bands appeared upon addition of EDC under the presence of mPEG5k-NH_2 or biotin-PEG5k-NH_2 (**Figures S13b, S13c**) indicating the covalent binding of PEG to the nanoparticles. In case of conjugating the particles with PEG the bands were completely retarded on the gel at high EDC concentrations. The negative control showed no significant non-specific binding of PEG without the presence of EDC. The attachment of one single PEG5k molecule seems to be sufficient to produce a significant shift of the fluorescent AuNC@DHLA leading to a discrete band on the gel.

In order to demonstrate the introduction of functionalities upon PEGylation, bands comprising fluorescent AuNC@DHLA conjugated with PEG5k-biotin were cut from the gel within the middle region of the band. Particles were recovered from the gel by diffusion out of the gel and further application of gel electrophoresis after transferring the gel pieces into a dialysis membrane of 8kDa MWCO. These fluorescent Au nanoclusters conjugated with PEG5k-biotins were then reacted with streptavidin to confirm the functionality of the biotin binding site. One streptavidin molecule can present up to four binding sites for biotin molecules. Here, we first dissolved streptavidin (salt-free, Sigma) in double distilled water. As shown in **Figure 14** fluorescent AuNC@DHLA without attached PEG-biotin showed negligible non-specific binding with streptavidin. On the other hand fluorescent AuNC@DHLA conjugated to PEG-biotin formed complexes with streptavidin which resulted in retarded bands on the gel. In this way it could be demonstrated that conjugation of biotin-PEG5k-amine to the surface of fluorescent Au nanoclusters did not hinder the function of biotin to binding streptavidin.

In a next step we demonstrate that proteins can be directly attached to the surface of fluorescent Au nanoclusters using EDC. First, avidin (Sigma; A9275) as example of a protein was suspended in double distilled water to a final concentration of 1 mg/ml. 128 mM EDC solution (Sigma) in double distilled water was prepared and aliquoted in seven fractions, out of which fraction contained one fourth of the EDC concentration compared to the previous fraction. EDC (10 µl) was added into mixture containing fluorescent AuNC@DHLA (10 µl, 15µM in SBB-pH7.4) and avidin (10 µl). After two hours reaction the fluorescent AuNC@DHLA were run through gel electrophoresis with 2% agarose gels (20 min, 7.5V/cm, Sub-Cell GT electrophoresis cells, Bio-Rad). As shown in **Figure S15**, the fluorescent AuNC@DHLA which have been reacted with high amounts of EDC in absence of avidin are aggregated and do not move on the gel. In contrast, upon the presence of avidin one discrete retarded band appeared on the gel upon addition of EDC. Furthermore, streptavidin showed a similar behavior as avidin (**Figure S16**). The streptavidin (Sigma S4762) was mixed with fluorescent AuNC@DHLA in the presence of EDC at two selected concentrations. Comparing with negative control (AuNC@DHLA plus EDC only), fluorescent gold nanoclusters reacting with streptavidin could be separated as a discrete band upon running the agarose gel electrophoresis. Obviously, only streptavidin-conjugated AuNC@DHLA contributes the retarded band due to its increase size, in the same way as AuNC@DHLA-avidin conjugates.

Gel electrophoresis has been used here as a facile way for confirming the attachment of big molecules containing primary amine to fluorescent Au nanoclusters by measuring changes in the migration speed upon attachment of the molecules. We

have also observed that a PEG-shell around the fluorescent AuNC@DHLA dramatically increases their colloidal stability for long-term storage, assessed by centrifugation.

SI.5: Labeling of living & fixed cells

SI.5-1 Non-specific labeling of living cells:

Like many other types of colloidal nanoparticles also fluorescent AuNC@DHLA are nonspecifically ingested by different types of cells. As demonstration human aortic endothelial cells (HAEC) were maintained in medium 200 with low serum growth supplement (all from Cascade Biologics). The culture was seeded onto 2% gelatin-coated glass coverslips and maintained in an incubator under a humidified 95% air and 5% CO_2 37 °C atmosphere. For incubation with fluorescent AuNC@DHLA HAEC cells were grown in condition medium 200 and serially passaged until they reached passage 8. Fluorescent gold nanoclusters were added to the culture medium (containing serum and antibiotics) and condition medium (serum and antibiotics free medium). After 5 hours of incubation the uptake of AuNC@DHLA was tested. For this purpose cells were fixed with 2% paraformaldehyde, washed with PBS, followed by bisbenzimide staining (18.7 μmol/l) of the nuclei for 15 min, washed with PBS, and finally immersed in 60% glycerol (v/v). Images were then recorded with an optical microscope (DM IRBE; Leica, DC 300F CCD camera, Leica). Fluorescence images were recorded with 340–380 / 425 nm and 515–560 / 590 nm excitation / emission for the visualization of bisbenzimide and fluorescent AuNC@DHLA, respectively. Results are shown in **Figure S17**. As no functionality had been introduced on the particle surface beside the carboxylic groups of DHLA, uptake of the AuNC@DHLA has to be considered as nonspecific.

SI.5-2 Specific labeling of fixed cells:

In contrast to non-specific uptake as demonstrated in SI.5-1 also specific labeling was investigated. For this purpose fluorescence AuNC@DHLA conjugated to avidin were used. Biotin, a vitamin essential for metabolism, is widely distributed in the body. Significant amount of endogenous biotin can be detected in rat kidney, liver and brain[6]. Therefore AuNC@DHLA-avidin conjugates should bind specifically to cells comprising endogenous biotin.

For the synthesis of avidin-conjugated AuNC@DHLA 1 ml of EDC in double distilled H_2O was added to a mixture of fluorescence AuNC@DHLA (15 μM, 1 ml) and avidin (1 mg/ml, 1 ml) and the mixture was reacted for two hours. In order to remove unconjugated AuNC@DHLA and unreacted avidin the reaction mixture was centrifuge in a 100 kDa MWCO Amicon centrifuge filter (Millipore). Non-reacted AuNC@DHLA as

well as avidin passes through the membrane, whereas the AuNC@DHLA with attached avidin could not pass the membrane. After several runs of washing, the fluorescent AuNC@DHLA-avidin conjugates were concentrated with the centrifuge filters to a volume of 200 ul in sodium borate buffer (SBB, pH 9). Fluorescence-labeled avidin, in particular FITC-Avidin (Pierce), was used as positive control. As negative control PEG10k-amine (3 mM, M=10,000 g mol^{-1}, Rapp polymere) was attached to the particles instead of avidin. These control particles should not exhibit any affinity to biotin.

Human hepatoma cell lines ($HepG_2$ cells) were obtained from the Bioresource Collection and Research Center (BCRC, Food Industry Research and Development Institute, Hsin Chu, Taiwan). Cells were grown in Dulbecco's modified Eagle's medium (DMEM), supplemented with 10% fetal bovine serum, 100 units/ml penicillin, 100 μg/ml streptomycin, 0.37% (w/v) $NaHCO_3$, 0.1 mM NEAA, 1 mM sodium pyruvate, 0.03% L-glutamine, and were maintained in an incubator (37 °C) under a humidified 95% air and 5% CO_2 atmosphere. For passaging $HepG_2$ cells with 90~95% confluence were detached with 0.1% trypsin and 10 μM EDTA in phosphate-buffered saline (PBS). Cells in passage 10 were sub-divided and seeded into 3-cm plastic culture dishes with 25000 cells/ dish. After 3 days of incubation cells were fixed by 2% paraformaldehyde (Sigma) in PBS, incubated with 0.5% Triton X-100 in PBS for 10 min, followed by nuclear staining using bisbenzimide (Hochest 33258, 18.7 μmol/l) for 15 min. After washing with PBS for several times, endogenous biotin within $HepG_2$ cells was probed using three conjugates: fluorescent AuNC@DHLA conjugated to PEG (negative control), fluorescent AuNC@DHLA conjugated to avidin, and fluorescent FITC-avidin (positive control). For this the PBS buffer was removed by aspiration and 30 μl of the AuNC@DHLA conjugates were added to the culture dish which was the covered by a coverslip to avoid evaporation. After 20 min incubation time cells were washed several times by PBS and then immersed in 60% glycerol (v/v). Images were then taken with a confocal laser scanning microscopy (LSM 510, Zeiss). As shown in **Figure S18**, fluorescent AuNC@DHLA-avidin conjugates and fluorescent FITC-avidin labeled the endogenous biotin in the human hepatoma cells. No labeling was observed to the fluorescent AuNC@DHLA conjugated to PEG.

Because PEGs are known as polymer which can reduce the nonspecific binding, we designed another experiment to confirm the difference between nonspecific and specific labeling in the fixed cells. Here the fluorescent AuNC@DHLA-streptavidin was selected as alternative for endogenous biotin labeling. FITC-labeled streptavidin (Sigma) were selected as positive control. Bare AuNC@DHLA and PEG- or BSA[xiv]-conjugated AuNC@DHLA were selected as testing of nonspecific labeling in the fixed $HepG_2$ cells. All probes were synthesized by following the previous strategy and adjusted the final concentration to 6 μM for labeling tests. After following the standard fixation, the

$HepG_2$ cells were immersed by 20 μl of different fluorescent probes for 10 minutes. An extra cover slip was used as cover to avoid sample drying. And then all the un-bounded nanoclusters were washed away by three times of PBS buffer. The final labeled cells that preserved in 60% glycerol (v/v) were imaged by confocal microscope under the same parameters setting. **Figure S19** showed both fluorescent images and phase image from each labeling. We found the bare AuNC@DHLA had some nonspecific labeling in the cell nucleus and similar results also happened in AuNC@DHLA-BSA. However, the nonspecific labeling was strongly reduced in group of fluorescent AuNC@DHLA-PEG, indicating that PEG is a good improvement in the probe design. Inversely, both fluorescent AuNC@DHLA- and FITC-labeled streptavidin showed an intense signal in the cell nucleus as well as the cytoplasm. From above results, we attribute the fluorescent signal mainly come from the labeling of endogenous biotin, but the existence of minor signals of nonspecific labeling (i.e. non-mapping to endogenous biotin) should be also concerned. Two ways might further solve this problem: one is to using the commercial available kits to reduce the rest of nonspecific binding and another is to link the PEG molecules on the un-reacted surface of fluorescent Au nanoclusters.

SI.6: References and notes

References

1. Jana, N. R.; Peng, X. G. *J. Am. Chem. Soc.* **2003,** 125, (47), 14280-14281.
2. Sperling, R. A.; Liedl, T.; Duhr, S.; Kudera, S.; Zanella, M.; Lin, C.-A. J.; Chang, W. H.; Braun, D.; Parak, W. J. *J. Phys. Chem. C* **2007,** 111, (31), 11552-11559.
3. Fee, C. J.; Alstine, J. M. V. *Bioconjugate Chem.* **2004,** 15, (6), 1304-1313.
4. Velapoldi, R. A.; Tonnesen, H. H. *J. Fluorescence* **2004,** 14, (4), 465-472.
5. Lin, C.-A. J.; Sperling, R. A.; Li, J. K.; Yang, T.-Y.; Li, P.-Y.; Zanella, M.; Chang, W. H.; Parak, W. J. *SMALL* **2008,** 4, (3), 334-341.
6. Wang, H.; Pevsner, J. *Cell Tissue Res.* **1999,** 296, 511-516.

Notes

[i] Oxidized forms of lipoic acids did not show reactive effects when introduced into solutions with etched gold nanocluster.

[ii] Basically, the AuNC@DHLA is hard to solubilize in chloroform.

[iii] Dried powders of DHLA-capped gold nanoclusters (AuNC@DHLA) without UV treatment were hard to dissolve in methanol, but well-soluble in 0.1 M NaOH.

[iv] The effective diameter of free PEG molecules can be estimated by the following formula: $d_{eff,PEG} = 0.03824\ M_w^{0.559}$. $d_{eff,PEG}$ is the hydrodynamic diameter in nm and M_w is the molecular weight of the PEG in g/mol or Da, resp.

[v] As mentioned the diameter of the inorganic core of the Au nanoclusters is 1.56±0.3 nm.

[vi] By assuming that charge effects can be neglected.

[vii] See SI.1-4.

[viii] Both types of particles were purified by passing them through a 100 KDa Amicon centrifuge filter and re-concentrated with 30 kDa Amicon centrifuge filters (Millipore).

[ix] For the synthesis protocols we refer to chapter SI.1.

[x] cf. the TEM analysis in chapter SI.2 (Figure S4).

[xi] We speculate that detaching DDAB surfactants might take away Au atoms from the nanoparticle surface.

[xii] There is fluorescence of $AuCl_3$ dissolved in DDAB solution, but there is no detectable fluorescence in other Au precursor such as $HAuCl_4$.

[xiii] Here we assumed the extinction coefficient to be 450000 $M^{-1}cm^{-1}$ at 420 nm.

[xiv] BSA: Bovine Serum Albumin from Sigma.

Figures:

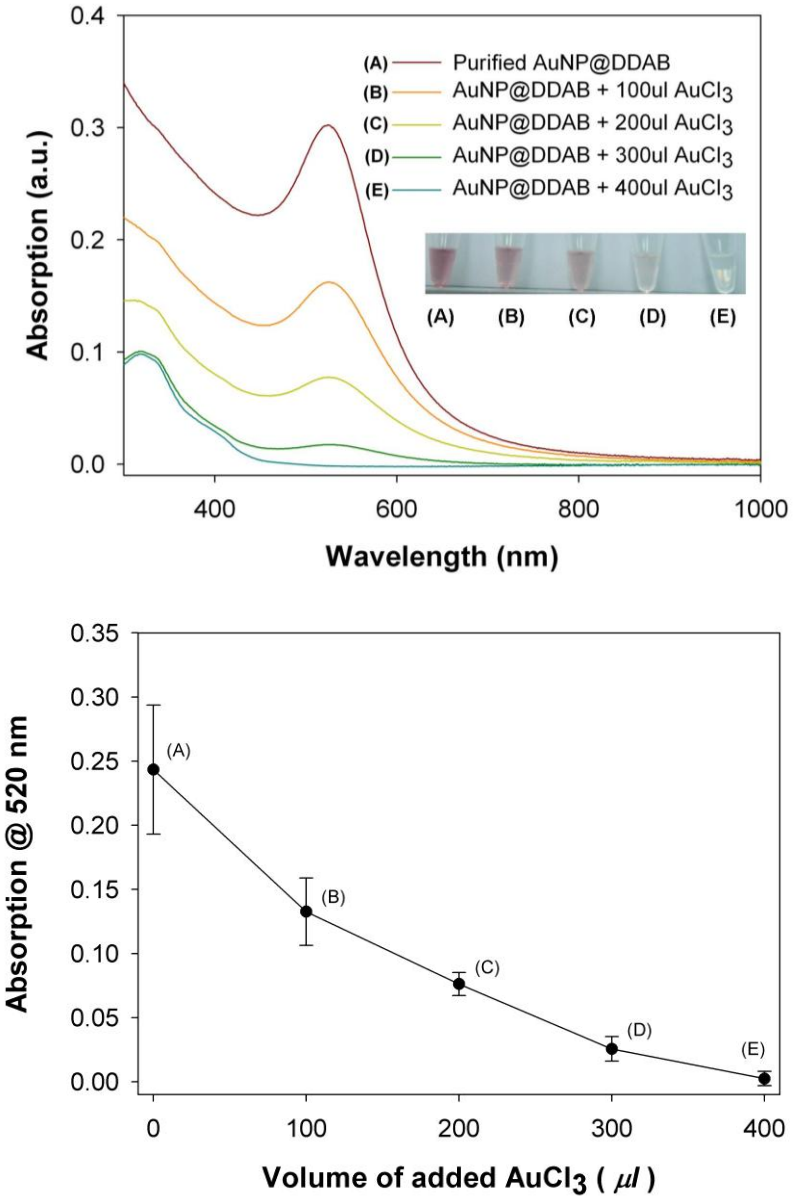

Figure S1. Etching of Au nanoparticles that had been purified with methanol precipitation. The 6-nm Au nanoparticles (AuNP@DDAB) synthesized via Peng's one-phase reaction were re-dispersed in 2.5 ml of DDAB solution upon methanol precipitation. Then 25 mM $AuCl_3$ precursor solution was added dropwise until the solution turned transparent. UV/vis absorption spectra were measured always when additional 100 μl of precursors had been added (See the upper figure. The image in the inset was taken after 50 times dilution of each aliquot). The plasmon absorption at 520 nm was plotted against the volume of added $AuCl_3$ solution (see the lower figure. The data points show mean values and error bars of three independent experiments). The results indicate that DDAB-stabilized Au nanoparticles are etched by addition of Au precursors.

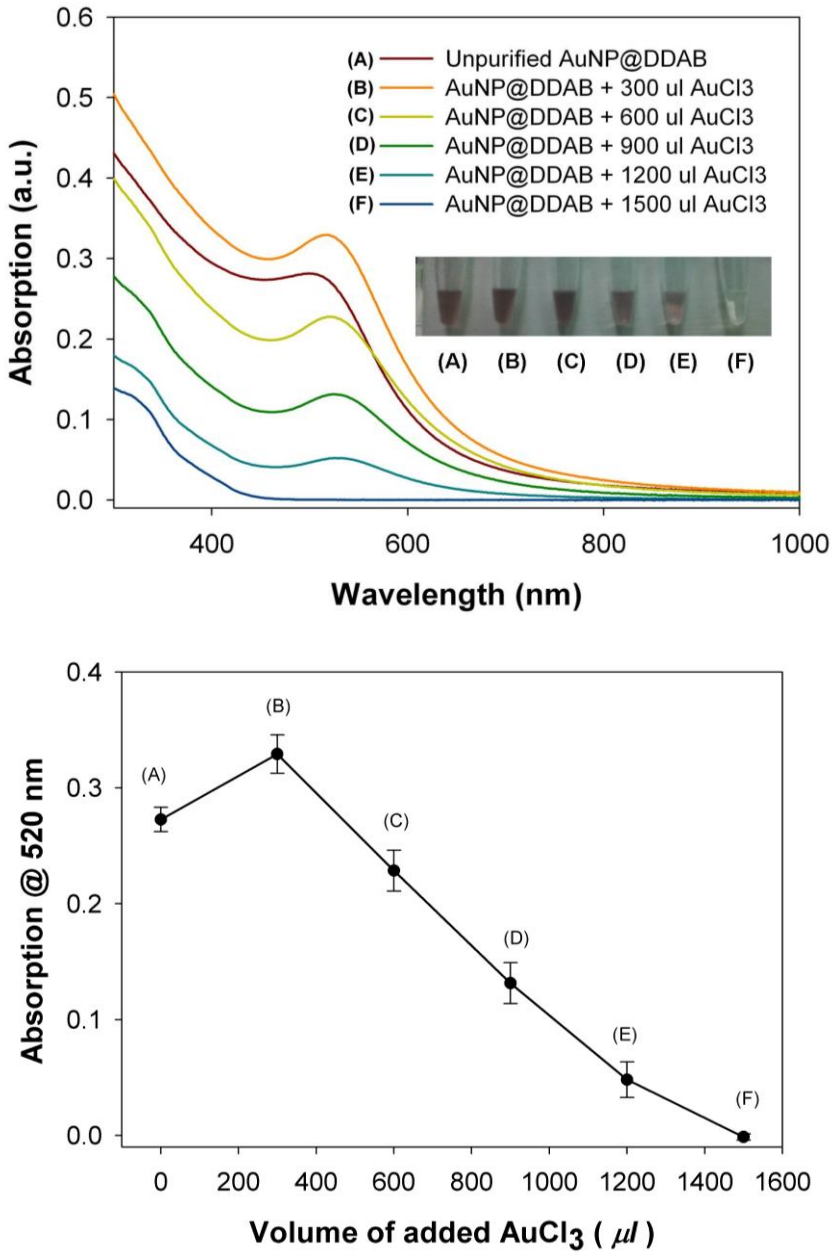

Figure S2. Etching of Au nanoparticles that had not been purified without methanol precipitation. The 6-nm Au nanoparticles (AuNP@DDAB) were synthesized via Peng's one-phase reaction procedure. After 2.5 min of reaction 25 mM $AuCl_3$ solution was added dropwise to the nanoparticle solution until the solution turned transparent. UV/vis absorption spectra were in intervals of 300 µl of added precursor solution (See upper figure. The image in the inset was taken after 50 times dilution of each aliquot). The plasmon absorption at 520 nm is plotted against the amount of added precursor solution (see the lower figure. The data points show mean values and error bars of three independent experiments). Upon addition of precursor solution the plasmon absorption initially increases and gradually disappears upon further addition of Au precursor solution.

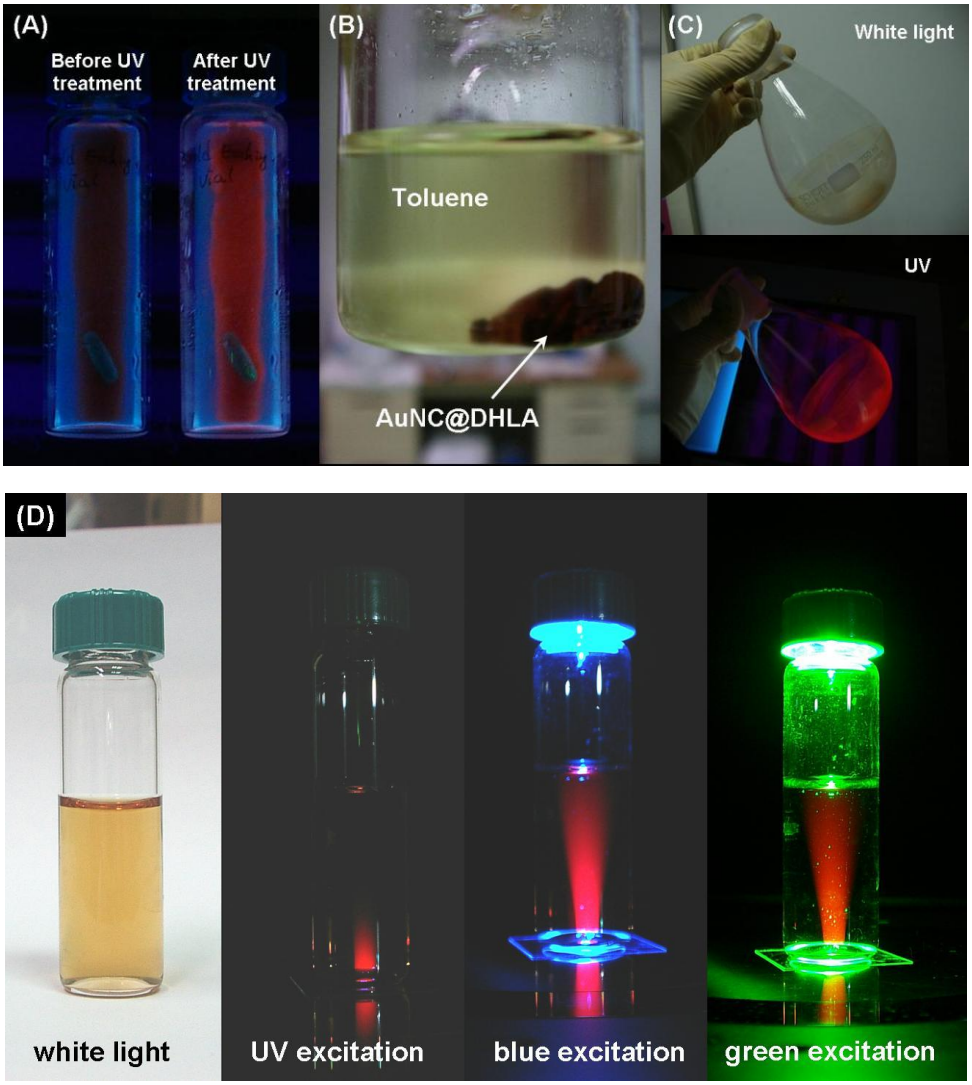

Figure S3. Fluorescent Au nanoclusters. Dihydrogenlipoic acid (DHLA) was added to the etched Au nanoclusters under vigorous stirring until a cloudy agglomerated solution appeared. (A) The red photoluminescence of the agglomerated Au nanoclusters (AuNC@DHLA) could be enhanced upon UV exposure. (B) AuNC@DHLA showed poor solubility in toluene. (C) After evaporating the solvent under reduced pressure, the dried film of Au nanoclusters was highly red-luminescent under UV light. (D) Upon addition of base (0.1 M NaOH), all nanoclusters were dispersed in the aqueous phase. Also the water-soluble Au nanoclusteres showed red photoluminescence at different excitation wavelengths as observed with a fluorescent microscope (Nikon TE300, Xenon lamp).

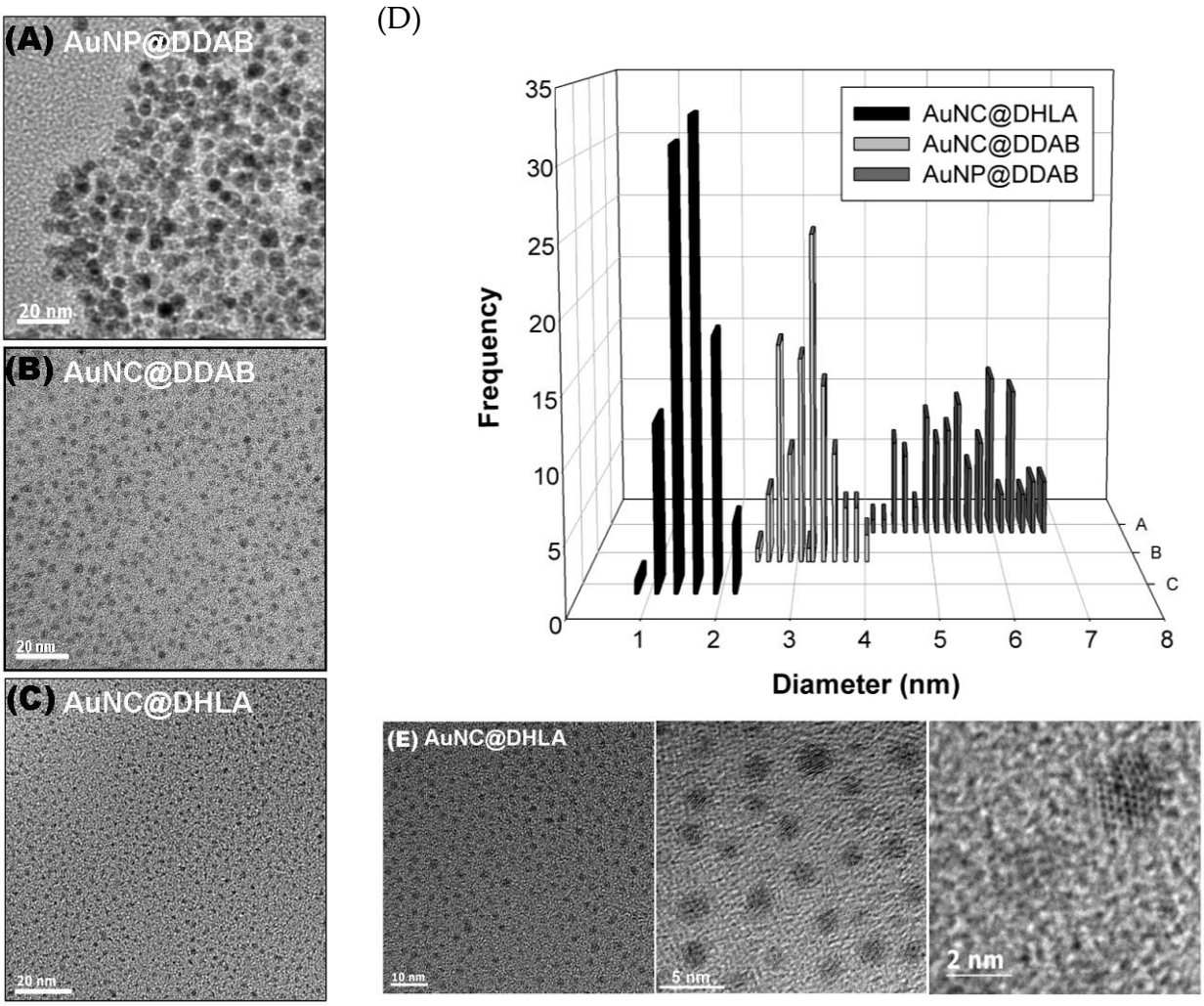

Figure S4. TEM imaging of different synthetic stages of fluorescent Au nanoclusters. The as-prepared Au nanoparticles were etched by adding $AuCl_3$ precursor solution until the plasmon absorption disappeared. To obtain water- and methanol-soluble samples the DDAB surfactant around the etched Au nanoclusters was replaced DHLA and the particles were exposed to UV (365 nm). All samples were diluted and directly added on carbon-coated TEM grids and the solvent evaporated to form a dry particle film. (A) 6-nm Au nanoparticles soluble in toluene (AuNP@DDAB); (B) etched Au nanoclusters soluble in toluene (AuNC@DDAB); (C) fluorescent Au nanoclusters soluble in methanol (AuNP@DHLA). Scale bars correspond to 20 nm. (D) The size distribution of Au particles was statistically analyzed by measuring the diameter of hundred particles and was found to be: (A). 5.55±0.68 nm, (B) 3.17±0.35 nm, and (C) 1.56±0.3 nm. (E) TEM images of fluorescent Au nanoclusters which were dispersed in methanol at different magnification (scale bars correspond to 10 nm, 5 nm, 2 nm).

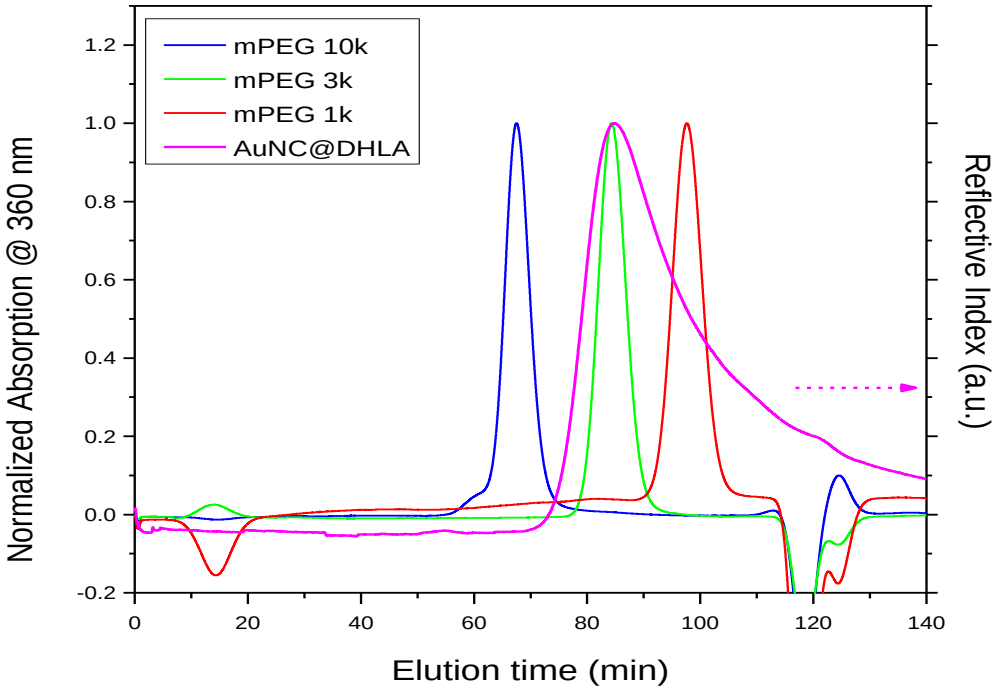

Figure S5. Size exclusion chromatography (SEC) elution profiles of fluorescent Au nanoclusters (AuNC@DHLA) compared with PEG standards. The absorption or reflective index of the eluted samples was plotted versus time. The larger the particles were, the faster they passed the column leading to shorter retention times. The fluorescent Au nanocluster samples possessed a distinguished absorption in the UV compared to the PEG standards which could be sensitively recorded by monitoring the refractive index. All samples were run on a Sephacryl S-200 column (72 cm x 15 mm ID) at 0.5 ml/min in 50 mM sodium borate buffer (100 mM NaCl, pH 9.0). The methoxy poly(ethylene glycol) (mPEG) molecules with different molecular weights (M_W 1kDa, 3kDa, 10kDa) showed different elution times, i.e. 67.52, 84.31 and 97.61 min (peak values), and corresponded to calculated diameters of 6.58, 3.36 and 1.82 nm, respectively. The elution time of the fluorescent Au nanoclusters (AuNC@DHLA) was observed at 84.79 min (peak value), its average elution time was located between the one of the 1 and 3 kDa PEG molecules.

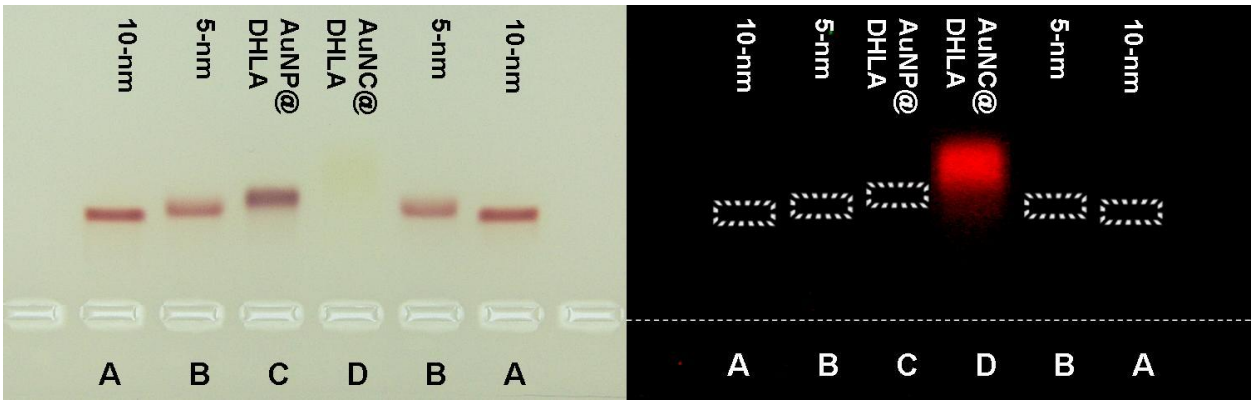

Figure S6. Gel electrophoresis of fluorescent gold nanoclusters (AuNC@DHLA) and gold nanoparticles (AuNP@DHLA). The Au nanoparticles synthesized by a one-phase reaction were etched into smaller nanoclusters via addition of Au precursors. Both types of hydrophobic nanoparticles (before and after the etching process) were then subject to ligand exchange with DHLA, leading to a negatively charged particle surface in alkaline buffers. After sequential purification steps, the DHLA-capped Au nanoparticles (C) and DHLA-capped Au nanoclusters (D) were run through 2% agarose gels (7.5V/cm, 20 min). Two reference samples (phosphine-coated 10 nm (A) and 5 nm (B) Au particles from BBI) were also loaded as reference. The gel pictures were recorded under visible light (left) as well as under UV 365 excitation (right).

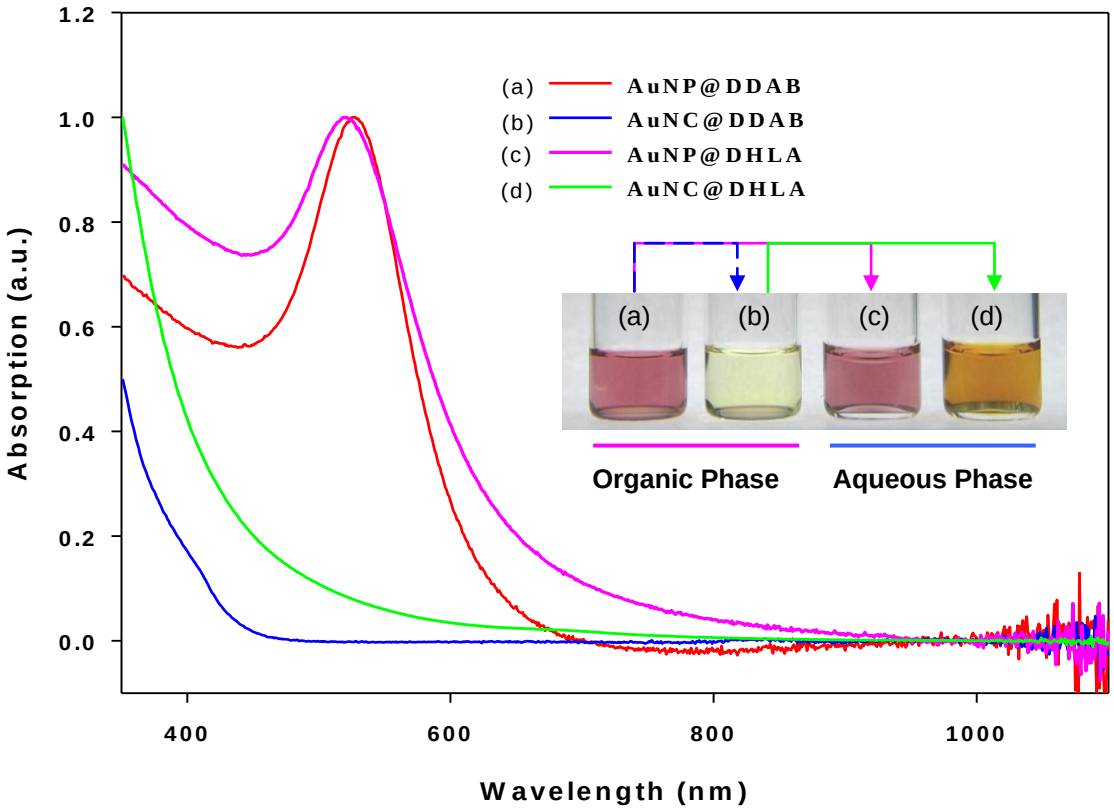

Figure S7. Absorption spectrum of Au nanoparticles and nanoclusters in organic and aqueous phase. The particles in organic solution are capped with DDAB surfactants, the particles in aqueous solution are capped with DHLA. (a) DDAB-capped Au NPs (AuNP@DDAB) show a strong surface plasmon absorption around 520~530 nm. (b) Plasmon absorption vanishes upon addition of Au precursor solution (25 mM $AuCl_3$ in DDAB solution), giving a etched gold nanoclusters (AuNC@DDAB). Both hydrophobic nanoparticles and nanoclusters were transferred into water phase via ligand exchange of dihydroxylipoic acid (DHLA). (c) DHLA-capped Au NPs (AuNP@DHLA) preserved their surface plasmon absorption, though a slight blue-shifted peak was observed. (d) The etched DHLA-capped Au NCs (AuNC@DHLA) showed an increasing absorption in the UV/vis range compared to the DDAB-capped Au NCs. The inset is photographic image of the four samples.

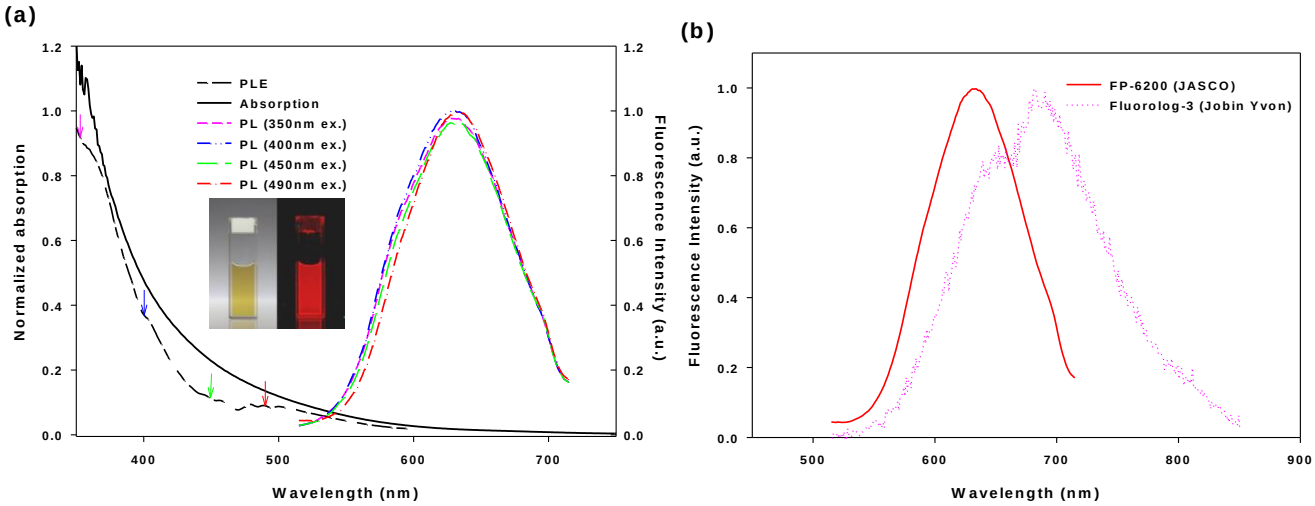

Figure S8. Absorption, photoluminescence (PL) and photoluminescence excitation (PLE) of fluorescent Au nanoclusters (AuNC@DHLA). (a) Optical absorption of diluted solutions of fluorescent AuNC@DHLA was measured with a fluorescence spectrometer (solid-line). The dash-line shows the corrected photoluminescence excitation (PLE) spectrum with observed emission at 630 nm. The related emission (PL) spectra of the fluorescent AuNC@DHLA excited by different wavelength (350, 400, 450, 490 nm) are plotted in colored dash-lines. Regardless the excitation wavelength the nanoclusters lead to a similar emission profile. PL and PLE data were recorded by a JASCO FP-6200 spectrometer. The inset picture shows a solution of fluorescent AuNC@DHLA under white-light and UV (365 nm) excitation. (b) Photoluminescence of fluorescent AuNC@DHLA dissolved in sodium borate buffer at 490 nm excitation was collected by two different fluorimeters (FP-6200, JASCO, 200~730 nm, and Fluorolog-3, Jobin Yvon, 200~850 nm), which offered different detection ranges. As emission of the fluorescent AuNC@DHLA is mainly located in the range of 600~800 nm the JASCO detector does not report the wavelength of maximum fluorescence correctly.

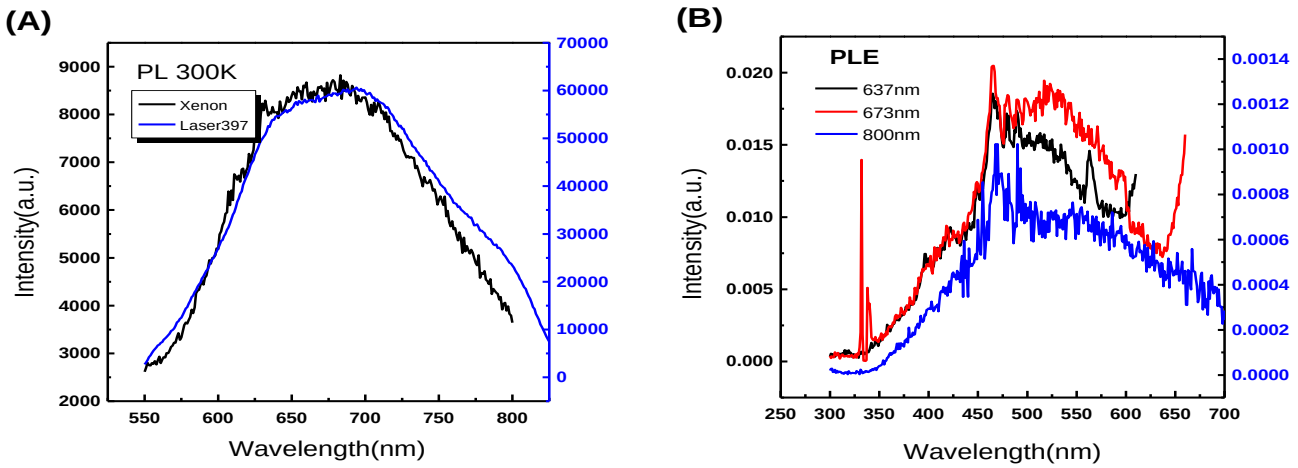

Figure S9. Solid-state photoluminescence (PL) and photoluminescence excitation (PLE) of fluorescent Au nanoclusters (AuNC@DHLA). A solution of fluorescent AuNC@DHLA dissolved in methanol was dried a glass coverslip, forming a thick particle layer on the glass surface. (A) The PL was collected using a GaN diode laser (396 nm) and a Xenon lamp (400 nm) as excitation source, which resulted to a similar peak profile of emission. (B) PLE recorded for emission at 637, 673, and 800 nm.

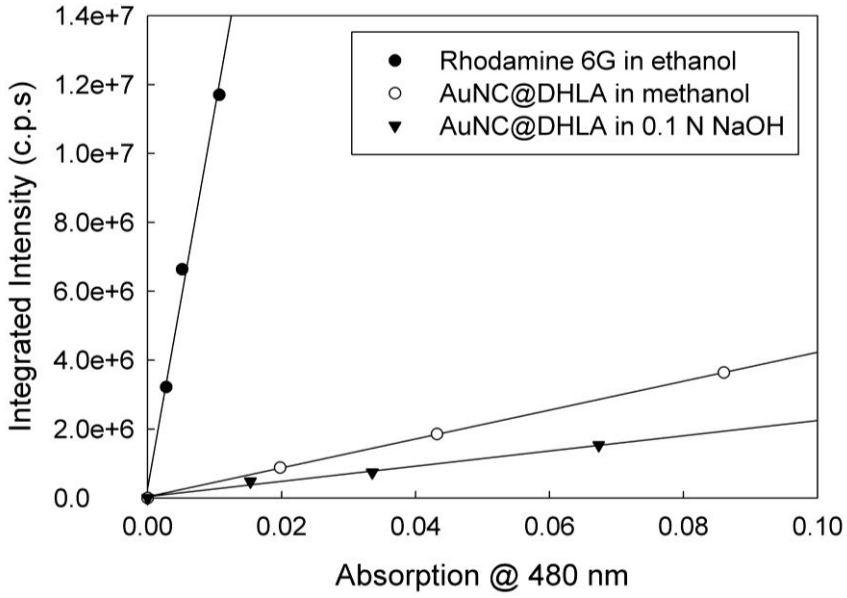

Figure S10. Quantum yield of the fluorescent gold gold nanoclusters (AuNC@DHLA). To calculate the quantum yield absorption and fluorescence spectra of concentration series of the test sample and a reference sample (with known quantum yield) were measured. The integrated intensity versus absorption of each sample was linearly fitted. Rhodamine 6G dissolved in ethanol (Q=0.95) was used as standard. Fluorescent AuNC@DHLA dispersed in methanol as well as in alkaline aqueous solution (0.1 N NaOH) were used. The quantum yield of fluorescent AuNC@DHLA was determined from the gradients as 3.45±0.41% in methanol and as 1.83±0.32% in aqueous phase.

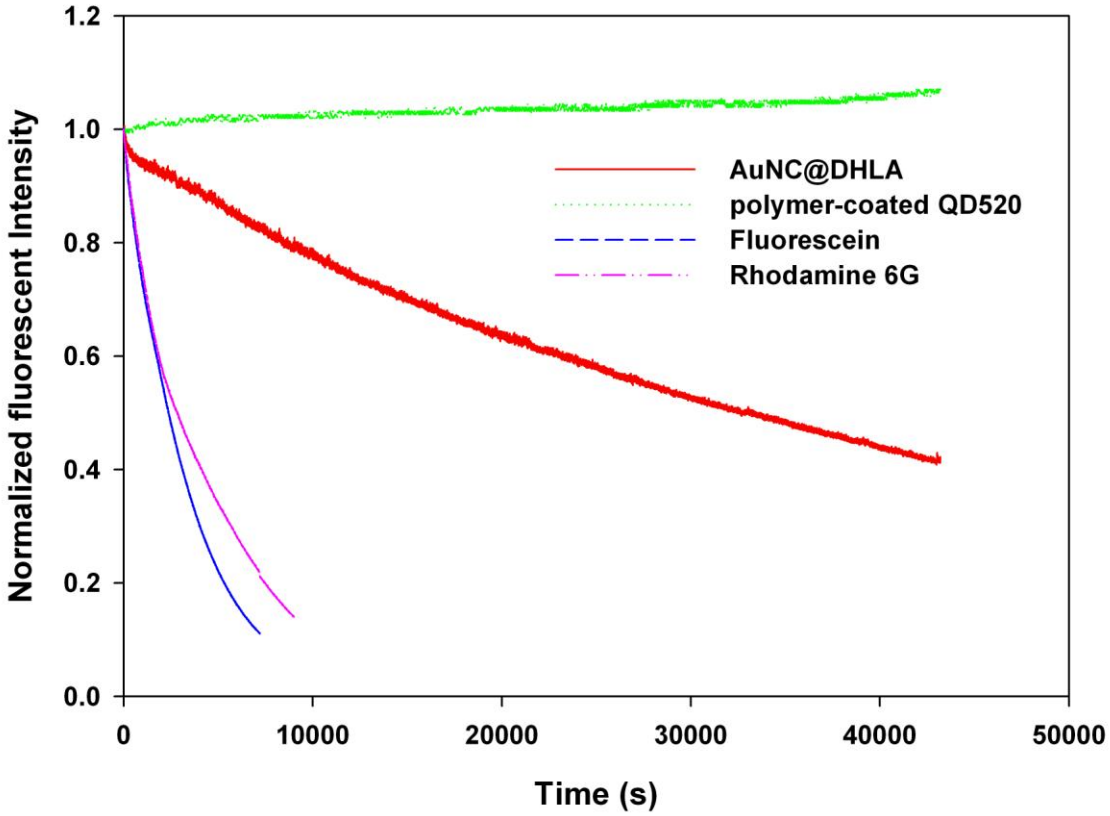

Figure S11. Photostability of fluorescent Au nanoclusters (AuNC@DHLA) compared to semiconductor quantum dots (polymer-coated QD 520 from Invitrogen) and organic fluorophores (fluorescein, Rhodamine 6G). 20 μl of fluorescent AuNC@DHLA dissolved in sodium borate buffer (pH 9) loaded into a quartz cuvette with small capacity were entirely exposed to blue-light (480 nm) excitation from the Xenon lamp of the used fluorometer (Fluolog-3, Jobin Yvon). Fluorescence intensity at 680 nm was recorded over time. Three water-soluble fluorescent materials, CdSe/ZnS quantum dots (polymer-coated QD520), Rhodamine 6G and fluorescein, were selected for comparison under the same excitation wavelength. All samples were adjusted to the same optical density at 480 nm before recording the PL intensity. The organic fluorophores show fast photobleaching, which is not present in the case of semiconductor quantum dots. The fluorescent Au nanoclusters exhibited a slower photobleaching rate than the organic fluorophores, though not as good as the semiconductor quantum dots. The half life of AuNC@DHLA in comparison to the organic dye is 32000s vs. 2500s respectively in the test condition.

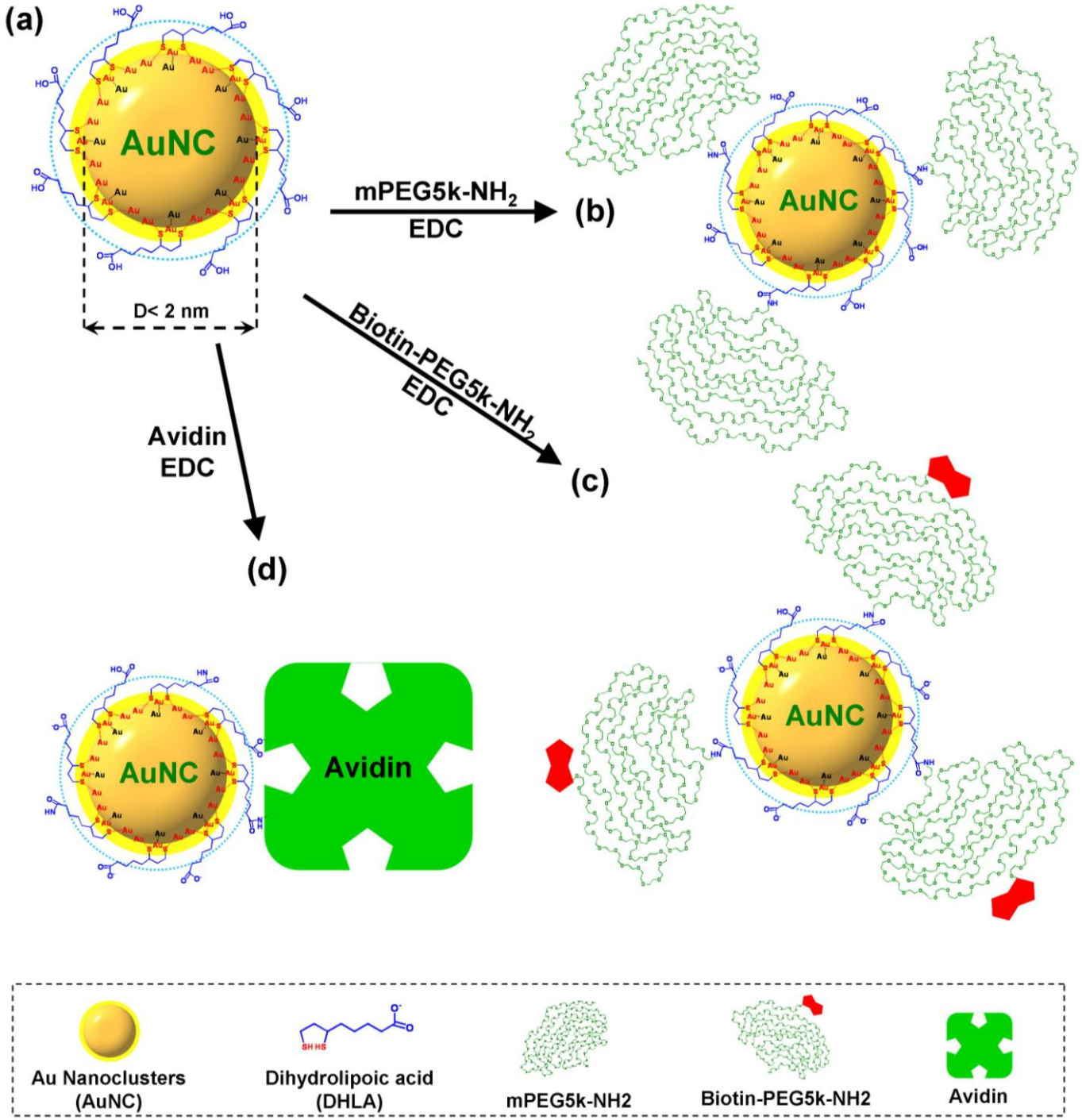

Figure S12. Illustration of the conjugation of fluorescent Au nanoclusters (AuNC@DHLA) with biomolecules (a) The pair of thiol groups of each dihydrolipoic acid (DHLA) molecule binds to the surface of Au nanoclusters, so that the carboxylic acids protrude into solution and thus provide water-solubility. The Au-core diameter of the fluorescent Au nanoclusters is around 0.5~2 nm. (Biological) molecules containing amine-groups can be covalently link to the carboxylic groups around the fluorescent AuNC@DHLA by EDC crosslinker chemistry. In the sketch linkage of three different (bio-)molecules is shown as example: (b) m-PEG5k-NH_2, (c) biotin-PEG5k-NH_2 and (d) avidin. Note that molecules are not drawn to scale.

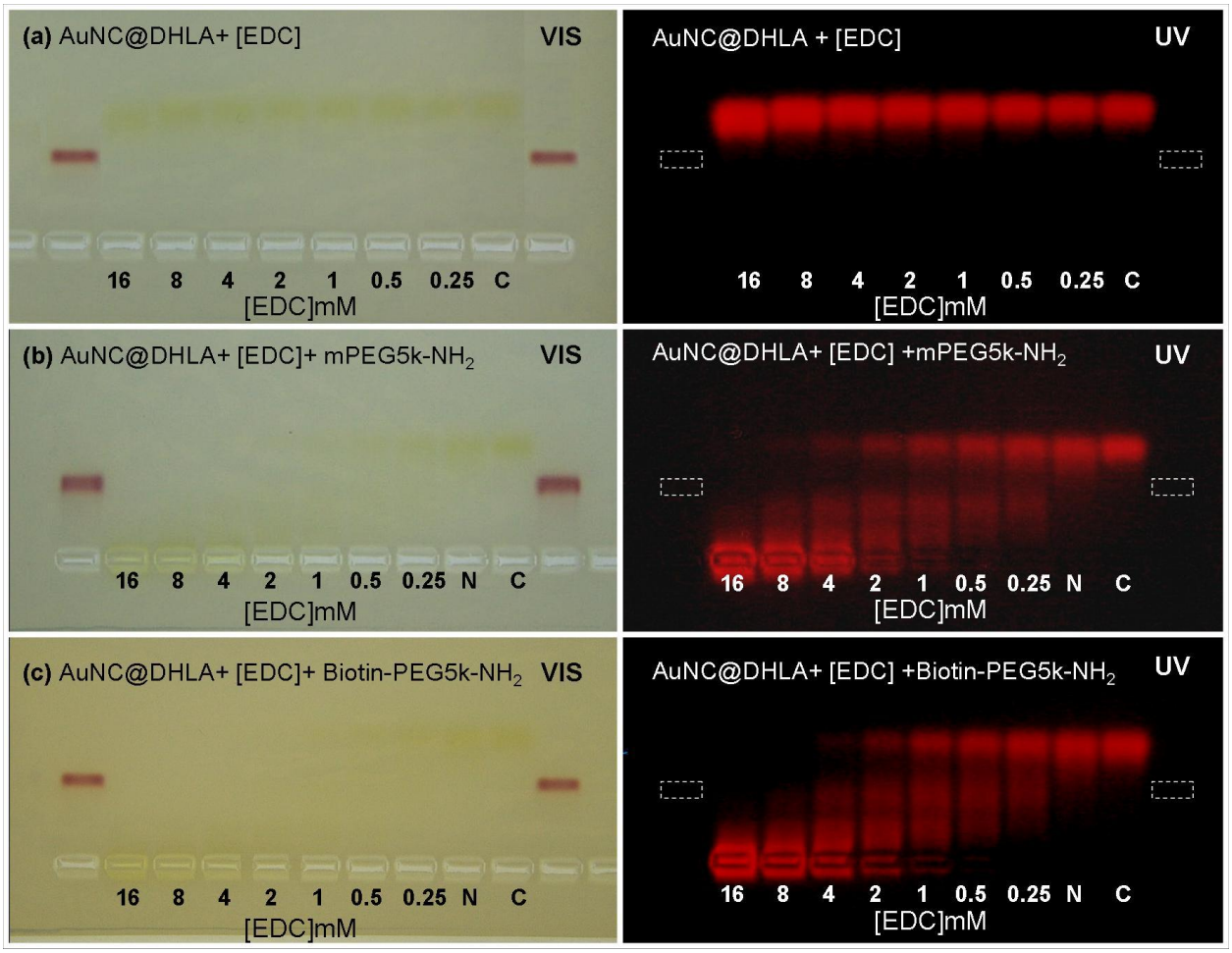

Figure S13. Gel electrophoresis for probing of the bioconjugation of fluorescent Au nanoclusters (AuNC@DHLA). 80 µl of 3 mM of PEG-amine (CH_3O-PEG-NH_2 or biotin-PEG-NH_2, M_W~5000 g/mol, Rapp Polymere) in double distilled H_2O were mixed with an equal volume of fluorescent AuNC@DHLA (15 µM) and split into aliquots of 20 µl each. To these samples, 10 µl of an EDC solution of appropriate concentration was added: c(EDC) = 0 (negative control "N"), 0.25, 0.5, 1, 2, 4, 8, and 16 mM. After 2 hours of reaction, the series of samples with different EDC concentration was run by gel electrophoresis (7.5 V/cm, 20 min) and photos of the gel were made under visible light (left) and UV lamp excitation (right). (a) The results from whole series without adding the PEG molecules; (b) whole series including mPEG-amine; (c) whole series including biotin-PEG-amine. As reference phosphine-coated gold nanoparticles (10 nm, BBInternational) were loaded into the first and last well. The more EDC had been added, the more PEG molecules were bound to the AuNC@DHLA and the more retarded the bands on the gel were. The lanes of the gels correspond to samples with increased EDC concentration from right to left. The functionality of the PEG terminus (methoxy- or biotin-group) does not have any significant difference for the conjugation procedure.

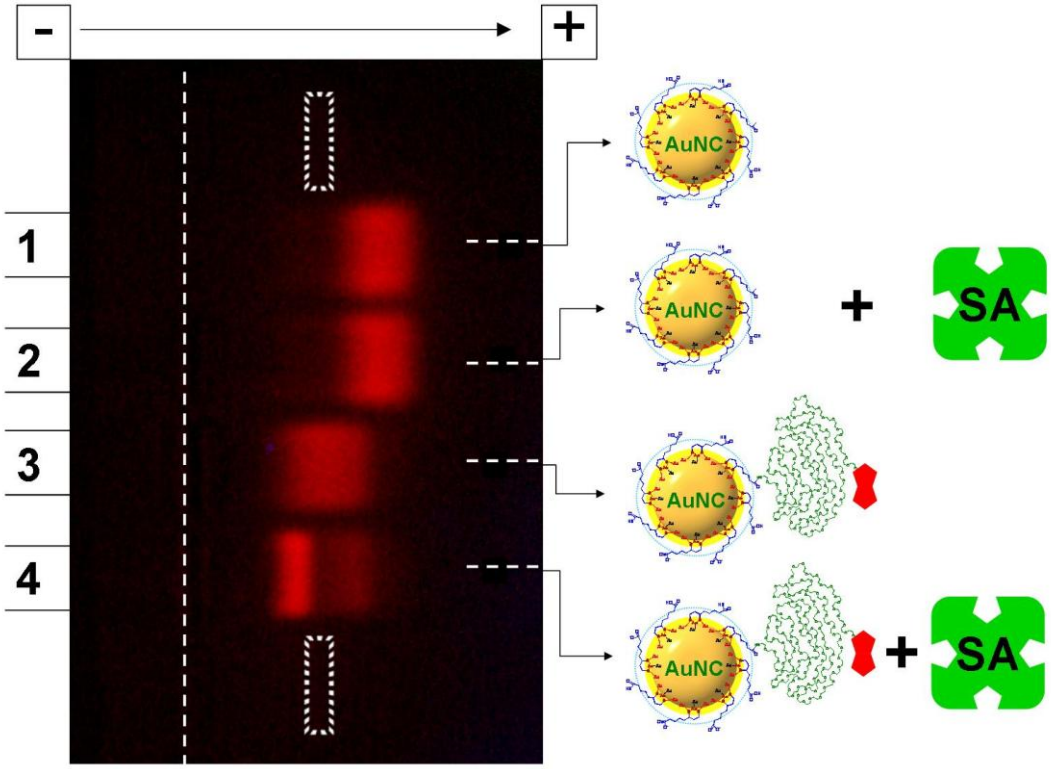

Figure S14. Probing of biotinylated fluorescent Au nanoclusters. Water-soluble fluorescent AuNC@DHLA were reacted with a mixture of EDC and biotin-PEG5k-amine for two hours (cf. Figure S13). After extraction from the gel and purification of the retarded bands which correspond to AuNC@DHLA with exactly one attached PEG5k-biotin molecule, these biotinylated AuNC@DHLA were reacted with streptavidin (1 mg/ml) in SBB-buffer (pH 9). Lane 1: unconjugated fluorescent AuNC@DHLA. Lane 2: unconjugated fluorescent AuNC@DHLA reacted with streptavidin. Lane 3: fluorescent AuNC@DHLA with covalently attached PEG5k-biotin. Lane 4: fluorescent AuNC@DHLA with covalently attached PEG5k-biotin reacted with streptavidin. The samples were run for 20 min on a 2% agarose gel (7.5 V/cm), including phosphine-coated gold nanoparticles (10-nm, dashed box) as reference. As can be seen the streptavidin did no show significant non-specific binding to the unconjugated Au NCs (lane 2). Addition of streptavidin to biotinylated AuNC@DHLA on the other hand lead to the appearance of an additional retarded band, which we attribute to a conjugation of biotinylated fluorescence Au NCs and streptavidin.

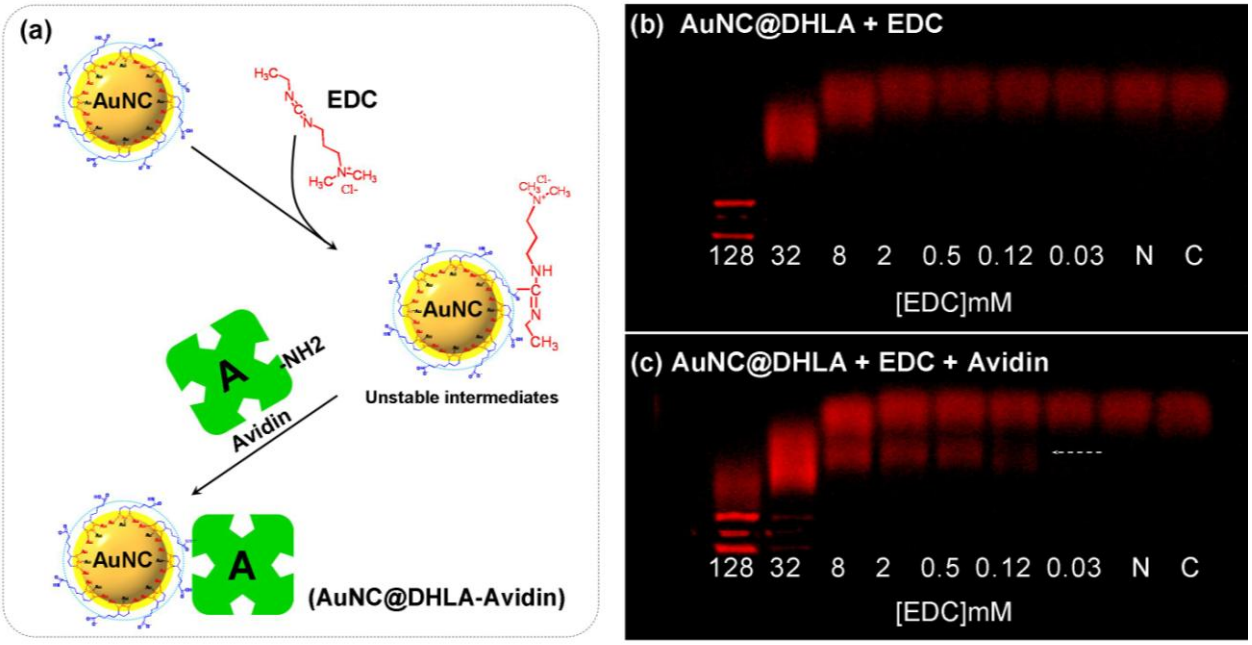

Figure S15. Gel electrophoresis of fluorescent Au nanoclusters with covalently attached avidin. As avidin molecules contain primary amino groups they could be also attached to surface of fluorescent AuNC@DHLA via crosslinkage to the COOH groups present of the particle surface using EDC. (a): EDC reacts with a carboxyl group present on the surface of fluorescent AuNC@DHLA by forming an amine-reactive *O*-acylisourea ester intermediate. This intermediate can react with primary amines present in avidin, yielding to AuNC@DHLA-avidin conjugates. In contrast to Figure S14 here avidin is covalently linked to the surfactant shell of the AuNC@DHLA without involving PEG as spacer. (b) Fluorescent AuNC@DHLA upon addition of EDC with different concentration (c(EDC) =128, 32, 8, 2, 0.5, 0.12, 0.03, 0 mM from left to right). (c) Fluorescent AuNC@DHLA upon addition of EDC with different concentration (c(EDC) =128, 32, 8, 2, 0.5, 0.12, 0.03, 0 mM from left to right) in the presence of avidin (1 mg/ml, Sigma, 2 hours reaction time). EDC at high concentration caused the retardation of the fluorescent AuNC@DHLA even when no avidin was present, which we attribute to an increasing number of *O*-acylisourea intermediates. However, under the presence of avidin a shifted band is visible already at lower EDC concentration which we attribute to the formation of conjugates of fluorescent AuNC@DHLA and avidin.

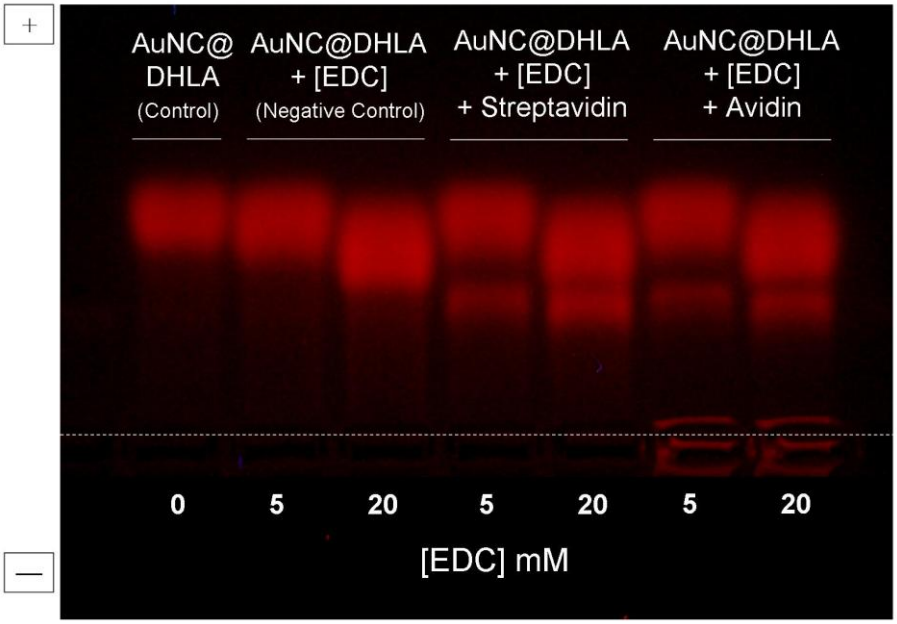

Figure S16: Gel electrophoresis of fluorescent Au nanoclusters with covalently attached streptavidin. As streptavidin molecules contain primary amino groups they could be also attached to surface of fluorescent AuNC@DHLA via crosslinkage to the COOH groups present of the nanoclusters surface using EDC. The loading samples from left to right on the gel are that fluorescent AuNC@DHLAs react with 0 (control), 5, 20 (negative) mM EDC as control and that the ones react with EDC (5, 20 mM) plus streptavidin or avidin (1 mg/ml) respectively. After running the samples on 2% agarose of gel electrophoresis (20 minutes), the band become broader and retarding when increasing the EDC from 0 to 20 mM, possibly caused by the formation of *O*-acylisourea ester intermediates. Only protein-containing samples show an additional shifted band, attributed to the formation of fluorescent AuNC@DHLA-streptavidin or AuNC@DHLA-avidin conjugates.

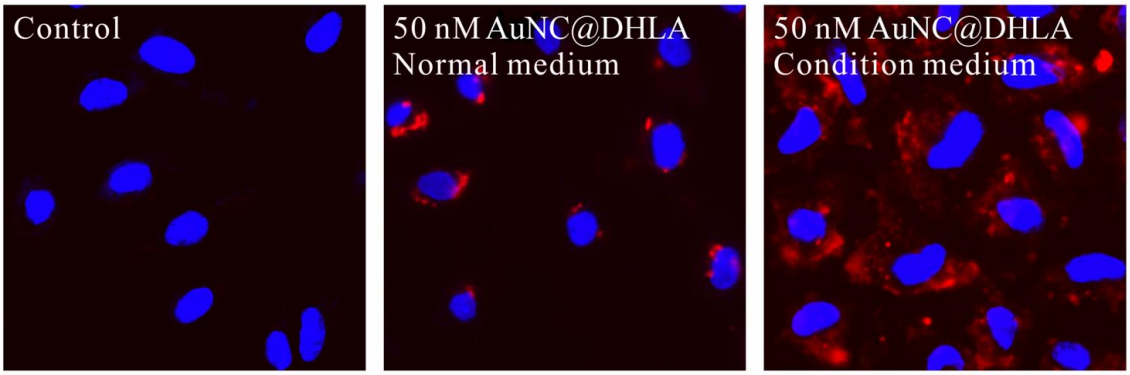

Figure S17. **Uptake of fluorescent Au nanoclusters by HAEC cells.** The red color corresponds to the fluorescent AuNC@DHLA and the blue color to stained cell nuclei. The concentration of added fluorescent AuNC@DHLA is denoted at the upper border of each image. (a) Cells without addition of fluorescent AuNC@DHLA (control). (b) Cells grown in normal culture medium upon the addition of fluorescent AuNC@DHLA. (c) Cells grown in condition medium without presence of serum. Scale bars correspond to 50 μm.

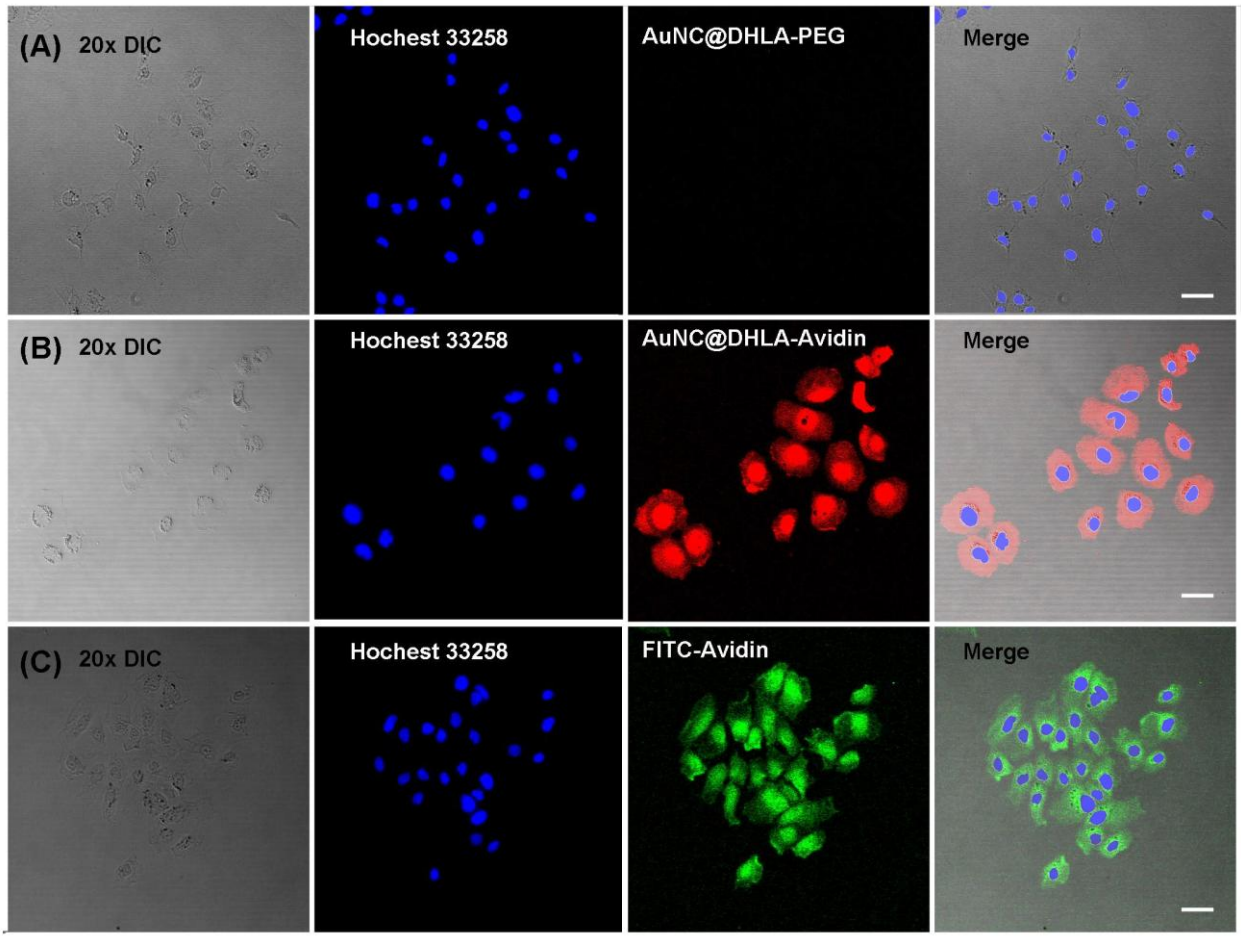

Figure S18. Labeling of endogenous biotin within a human hepatoma ($HepG_2$) cell lines with fluorescent Au nanoclusters (AuNC@DHLA) and controls. The following markers were added to the cells: (A) AuNC@DHLA conjugated with PEG as negative control. (B) AuNC@DHLA conjugated with avidin. (C) FITC-labeled avidin as positive control. The cell images from left to right are: transmission light image, staining of the nuclei, labeling of endogenous biotin as visualized by the fluorescence of Au-NCs or FITC, merged image. All images were recorded with a 20x objective (PLAN NEOFLUAR). Nuclei were stained by Hochest 33258 (UV excitation). Fluorescent Au-NCs were excited by with 514nm laser light. FITC was excited by 488 nm. The image demonstrate that avidin bound to fluorescent AuNC@DHLA behaves similar to FITC-labeled avidin. The scale bars correspond to 50 μm.

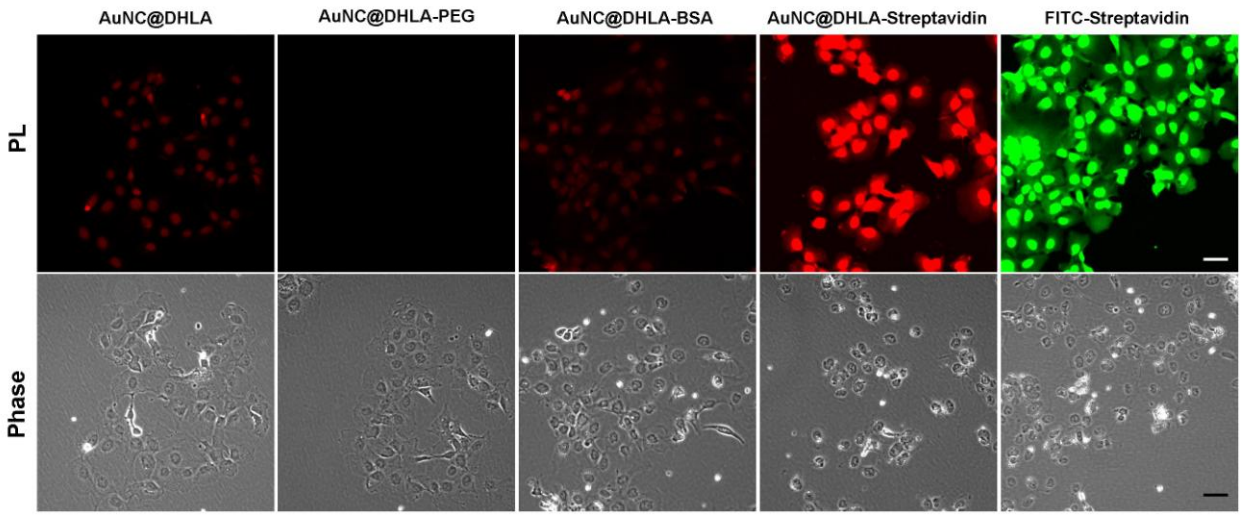

Figure S19. Labeling of endogenous biotin within a human hepatoma ($HepG_2$) cell lines with fluorescent Au nanoclusters conjugated to streptavidin (AuNC@DHLA-Streptavidin). Three negative controls were involved in the labeling testing: bare AuNC@DHLA, AuNC@DHLA-PEG, AuNC@DHLA-BSA from left, respectively. FITC-Streptavidin served as positive control in the right. All images were recorded with a 20x objective (PLAN NEOFLUAR) under Zeiss confocal microscope. Upper images are taken from fluorescent signal of each sample (AuNC@DHLA: LP 585 em/ 488 ex; FITC LP 530/ 488 ex). Lower images are the related phase images of $HepG_2$ cells from each labeling. Scale bare: 50 μm. This image demonstrated that the fluorescent AuNC@DHLA-linked streptavidin can specifically label the endogenous biotin in $HepG_2$ cells, consistent with the positive labeling using FITC-linked streptavidin. The low nonspecific binding existed in cells labeled by the bare AuNC@DHLA as well as AuNC@DHLA-BSA, but it was great reduced in cells labeled by AuNC@DHLA-PEG. The scale bars correspond to 50 μm.